

# Cosmic $e^\pm$ , $\bar{p}$ , $\gamma$ and neutrino rays in leptocentric dark matter models

<sup>1,2</sup>Xiao-Jun Bi, <sup>1,3</sup>Xiao-Gang He, <sup>4</sup>Ernest Ma, <sup>2</sup>Juan Zhang

<sup>1</sup>*Center for High Energy Physics, Peking University, Beijing 100871*

<sup>2</sup>*Laboratory of Particle Astrophysics, Institute of High Energy Physics,  
Chinese Academy of Sciences, Beijing 100049*

<sup>3</sup>*Department of Physics, Center for Theoretical Sciences,  
and LeCospa Center, National Taiwan University, Taipei*

<sup>4</sup>*Department of Physics, University of California, Riverside, California*

Dark matter annihilation is one of the leading explanations for the recently observed  $e^\pm$  excesses in cosmic rays by PAMELA, ATIC, FERMI-LAT and HESS. Any dark matter annihilation model proposed to explain these data must also explain the fact that PAMELA data show excesses only in  $e^\pm$  spectrum but not in anti-proton. It is interesting to ask whether the annihilation mode into anti-proton is completely disallowed or only suppressed at low energies. Most models proposed have negligible anti-protons in all energy ranges. We show that the leptocentric  $U(1)_{B-3L_i}$  dark matter model can explain the  $e^\pm$  excesses with suppressed anti-proton mode at low energies, but at higher energies there are sizable anti-proton excesses. Near future data from PAMELA and AMS can provide crucial test for this type of models. Cosmic  $\gamma$  ray data can further rule out some of the models. We also show that this model has interesting cosmic neutrino signatures.

PACS numbers: 98.80.Cq 11.15.Tk 11.25.Hf 14.80.-j

## I. INTRODUCTION

Recently several experiments have reported  $e^\pm$  excesses in cosmic ray (CR) energy spectrum. Last year the PAMELA collaboration reported  $e^+$  excess in the CR energy spectrum from 10 to 100 GeV, but observed no anti-proton excess [1, 2] compared with predictions from CR physics. These results are compatible with the previous HEAT and AMS01 exper-

iments (e.g., Ref. [3, 4]) but with higher precision. Shortly after the ATIC and PPB-BETS balloon experiments have reported excesses in the  $e^+ + e^-$  spectrum between 300 and 800 GeV [5, 6]. The ATIC data show a sharp falling in the energy spectrum around 600 GeV. Newly published result from FERMI-LAT collaboration also shows excesses in the  $e^+ + e^-$  energy spectrum above the background [7]. However, the spectrum is softer than that from ATIC. In addition, the HESS collaboration has inferred a flat but statistically limited  $e^+ + e^-$  spectrum between 340 GeV and 1 TeV [8] which falls steeply above 1 TeV [9]. These observational data have generated a lot of excitement as the excesses may be explained by dark matter (DM) annihilation or decay with appropriate properties [10, 11, 12, 13, 14].

If DM annihilation is responsible for the observed data, a lot of information can be extracted about DM properties[10, 11, 12, 13, 14]. The mass of the annihilating DM serves as the cut off scale of the  $e^\pm$  spectrum, the lepton spectra must have a cut off energy at the DM mass  $m_D$ . The FERMI-LAT and HESS data would require that the DM mass to be around a few TeV. The DM belongs to the weakly interacting massive particle (WIMP) category. The fact that PAMELA did not see anti-proton excess indicates that the DM is hadrophobic or leptophilic. At least hadronic annihilation modes are suppressed. Also since the same DM annihilation rate producing the  $e^\pm$  excesses is related to the annihilation rate producing the cosmological relic DM density, 23% of the energy budget of our universe, the annihilation rate is constrained. The latter requires that the thermally averaged annihilation rate  $\langle\sigma v\rangle$  to be  $3\times 10^{-26} \text{ cm}^3\text{s}^{-1}$ . If this annihilation rate is used to calculate the  $e^\pm$  spectrum, it is too small by a factor of 100 to 1000. There is the need to boost up the spectrum with a boost factor  $B$  of 100 to 1000. Any DM model proposed to explain the data should be able to produce the large boost factor too.

To suppress the cosmic anti-protons leptophilic DM models are proposed by several authors [12, 13]. In this type of models the DM only interacts with leptons in the standard model (SM). However, these DM models are hard to be tested since DM does not interact with hadrons at all. Another widely considered  $U(1)$  extension of the SM is the gauged B-L. However, if DM interacts with the SM with the gauged  $U(1)_{B-L}$  interaction too much anti-protons will be produced and therefore in conflict with PAMELA data. In this work, we propose a particle physics DM model, the gauged [15]  $U(1)_{B-3L_i}$  DM model, to explain the  $e^\pm$  excess data. Here B is the baryon number and  $L_i$  is one of the  $e$ ,  $\mu$  and  $\tau$  lepton numbers.

In this model, the DM is a Dirac fermion with nontrivial  $U(1)_{B-3L_i}$  charge [15]. The gauge boson of this  $U(1)$  group,  $Z'$ , mediates DM annihilation into SM particles. This model is not a pure leptophilic DM model, like the  $U(1)_{L_i-L_j}$  model studied in Ref. [13]. But has larger couplings to leptons than quarks. We refer it as the leptocentric dark model. The  $Z'$  has suppressed couplings to quarks leading to suppressed anti-proton up to the PAMELA energy reach, but may lead to excesses at higher energies. With the  $Z'$  mass close to two times of the DM mass, a large boost factor can be produced through the Breit-Wigner enhancement mechanism [11, 16]. The shape of the  $e^\pm$  spectrum helps to further constrain the choice of the lepton flavor  $L_i$  of the  $U(1)_{B-3L_i}$ .

All DM annihilation models proposed to explain  $e^\pm$  contribute at certain level to  $\gamma$ -rays by final state radiation. One must check if the model is compatible with available data. We find that for the  $L_i = \tau$  model, the hadronic  $\tau$  decays lead to too much  $\gamma$ -rays in conflict with data and only the  $L_i = L_{e,\mu}$  models can pass the  $\gamma$  ray data constraint if one takes the  $e^\pm$  excess spectrum to fit the ATIC or FERMI-LAT data. It is interesting to note that the  $Z'$  has the same couplings for charged lepton  $l_{L_i}$  and neutrino  $\nu_{L_i}$ . Therefore after fitting data on  $e^\pm$  excesses in CR, the cosmic neutrinos by DM annihilation from the Galactic center (GC) are predicted. The neutrino signals can be tested by experiments such as IceCube.

In the next section we will first describe how to treat the propagation of charged cosmic rays in the Milky Way. Then we present the leptocentric  $U(1)_{B-3L_i}$  DM model in Sec. III. The cosmic  $e^\pm$ ,  $\bar{p}$ ,  $\gamma$  and neutrino spectra predicted are given in Sec. IV, V, VI and VII respectively. Finally we give our conclusions in Sec. VIII.

## II. THE PROPAGATION MODELS

Before detailed studies of the CRs from the leptocentric  $U(1)_{B-3L_i}$  DM model, let us first briefly describe the CR propagation model which predicts the positron and anti-proton spectra to compare with data, and also  $\gamma$  and neutrino CRs.

The charged particles propagate diffusively in the Galaxy due to the scattering with random magnetic field[17]. The interactions with interstellar media (ISM) and interstellar radiation field (ISRF) will lead to energy losses of CRs. For heavy nuclei and unstable nuclei there are fragmentation processes by collisions with ISM and radioactive decays respectively. In addition, the overall convection driven by the Galactic wind and reacceleration due to

the interstellar shock will also affect the propagation processes of CRs. The propagation equation can be written as[18]

$$\begin{aligned} \frac{\partial \psi}{\partial t} = & Q(\mathbf{x}, p) + \nabla \cdot (D_{xx} \nabla \psi - \mathbf{V}_c \psi) + \frac{\partial}{\partial p} p^2 D_{pp} \frac{\partial}{\partial p} \frac{1}{p^2} \psi \\ & - \frac{\partial}{\partial p} \left[ \dot{p} \psi - \frac{p}{3} (\nabla \cdot \mathbf{V}_c \psi) \right] - \frac{\psi}{\tau_f} - \frac{\psi}{\tau_r}, \end{aligned} \quad (1)$$

where  $\psi$  is the density of cosmic ray particles per unit momentum interval,  $D_{xx}$  is the spatial diffusion coefficient,  $\mathbf{V}_c$  is the convection velocity,  $D_{pp}$  is the diffusion coefficient in momentum space used to describe the reacceleration process,  $\dot{p} \equiv dp/dt$  is the momentum loss rate,  $\tau_f$  and  $\tau_r$  are time scales for fragmentation and radioactive decay respectively. Here  $Q(\mathbf{x}, p)$  is the source term. For the astrophysical sources they are located within the Galactic disk [18, 19] while for DM annihilation the source is within the whole dark matter halo. The source term of DM annihilation is given as

$$Q(\mathbf{X}, E) = \frac{\langle \sigma v \rangle}{2m_\chi^2} \frac{dN}{dE} \rho^2(\mathbf{X}), \quad (2)$$

with  $\langle \sigma v \rangle$  the annihilation cross section and  $m_\chi$  the mass of dark matter particle,  $dN/dE$  the spectrum per annihilation and  $\rho(\mathbf{X})$  the dark matter density at  $\mathbf{X}$ .

The spatial diffusion is regarded as isotropic and described using a rigidity dependent function  $D_{xx} = \beta D_0 \left( \frac{\rho}{\rho_0} \right)^\delta$  with  $\rho$  the rigidity of the particles. The reacceleration is described by the diffusion in momentum space with the diffusion coefficient  $D_{pp}$ , which relates with the spatial diffusion coefficient  $D_{xx}$  as shown in [20]. The convection velocity is cylindrically symmetric and increases linearly with the height  $z$  from the Galactic plane[18]. Finally the energy losses and fragmentations are calculated according to the interactions between CRs and the interstellar gas or the interstellar radiation field.

A numerical method to solve Eq. (1) has been developed by Strong and Moskalenko, known as the GALPROP model [18]. In GALPROP, the realistic astrophysical inputs such as the interstellar medium (ISM) and interstellar radiation field (ISRF) are adopted to calculate the fragmentations and energy losses of CRs. The parameters are tuned to reproduce all the observational CR spectra at Earth. The GALPROP model can give very good descriptions of all kinds of CRs, including the secondaries such as  $e^+$ ,  $\bar{p}$  and diffuse  $\gamma$ -rays[18, 21, 22, 23].

In this work we employ GALPROP to calculate the propagation of CRs. We will adopt the diffusion + convection (DC) scenario with parameters given in Ref. [19]. The DC model

predicts the  $e^-$ ,  $e^+$ ,  $p$  and  $\bar{p}$  spectra with very good agreement with the data [18].

The main uncertainty of the propagation model comes from the height of the Galactic diffusion region. If the height is changed the diffusion coefficient can be adjusted accordingly so that the confinement time of the cosmic particles within the Galaxy and the secondary products are kept intact. However, such adjustments affect the contribution from DM annihilation greatly [24]. The reason is that the sources of CRs are located within the thin Galactic disk, which is much smaller than the diffusion region no matter how to adjust the height. But the contribution from DM annihilation comes from the whole dark matter halo. Only when the annihilation takes place within the diffusion region can it contribute to the observed cosmic ray fluxes. The particles from the region out of the diffusion region escape freely. Therefore the height affects the contribution of DM annihilation greatly.

The effects by changing the diffusion height are also different for electrons and nuclei from DM annihilation. For electrons and positrons the main effects that affect their spectra are the energy loss processes, such as the synchrotron radiation or inverse Compton scattering with the ISRF. Since electrons/positrons loss energy rapidly, the high energy electrons can not propagate for long distance, usually smaller than 1kpc [25]. On the contrary the nuclei are mainly affected by the propagation processes and propagate much longer than the electrons and positrons. Therefore the diffusion height affects anti-proton contribution by DM annihilation much more than positrons. In the following we will try to adjust the diffusion height to suppress the anti-proton contribution from DM annihilation while the electrons/positrons can fit the PAMELA and Fermi data at the same time.

In the conventional cosmic ray model the diffusion height  $Z_h$  is taken as 4kpc, which can give best fit to all CR data. Considering the data from diffuse  $\gamma$ -rays the height should be at least of about  $\sim 2$ kpc. In our calculation we will take another set of propagation parameters with the height  $Z_h = 2$ kpc. All other parameters are adjusted correspondingly to fit the CR data.

For cosmic  $\gamma$ - or neutrino-rays, since they can propagate freely in the Galaxy, one can obtain their fluxes by simply integrating the source terms along the line of sight (LOS) at any direction. The flux  $\phi(E_{\gamma,\nu})$  for  $\gamma$  and neutrino are given by

$$\phi(E_{\gamma,\nu}, \psi) = \frac{1}{4\pi} \times \frac{\langle \sigma v \rangle}{2m_\chi^2} \frac{dN}{dE_{\gamma,\nu}} \times \int_{LOS} \rho^2(l) dl, \quad (3)$$

where  $\phi(E_{\gamma,\nu}, \psi)$  are the  $\gamma$ - and neutrino-ray spectra at the direction  $\psi$  and  $dN/dE_{\gamma,\nu}$  are the

$\gamma$ - and neutrino-ray spectra per annihilation, respectively. For the emission from a diffuse region with solid angle  $\Delta\Omega$ , we define the average flux as

$$\phi_{\Delta\Omega} = \frac{1}{\Delta\Omega} \int_{\Delta\Omega} \phi(\psi) d\Omega . \quad (4)$$

In the rest of the sections, we will follow the above prescriptions to calculate the  $e^\pm$ , anti-proton,  $\gamma$  and neutrino CRs in the  $U(1)_{B-3L_i}$  models.

### III. THE LEPTOCENTRIC $U(1)_{B-3L_i}$ DARK MATTER MODEL

Data from PAMELA show that there are excesses in cosmic  $e^\pm$  energy spectrum, but not in anti-proton spectrum. This prompts several authors to propose leptophilic DM models [12, 13]. The simplest leptophilic model is the gauged  $U(1)_{L_i-L_j}$  DM model [13]. In the minimal SM, besides the  $SU(3)_C \times SU(2)_L \times U(1)_Y$  gauge groups, the family lepton number difference  $L_i - L_j$  can be gauge without anomaly. The resulting  $Z'$  coupling to SM particles are leptophilic. Among the three possible models, two of the models  $L_e - L_\mu$  and  $L_e - L_\tau$  can explain the PAMELA and ATIC data well, while the  $L_\mu - L_\tau$  model can fit PAMELA, FERMI and HESS data well and disfavor the other two models. This model leaving very little signal in hadronic mode. The anti-proton excess is suppressed at a negligible level for all ranges of anti-proton energies.

With right handed neutrinos, one can gauge the  $B - L$  global symmetry without gauge anomalies. This model has also been studied in the context of the recent  $e^\pm$  excesses. However, in this type of models, the  $Z'$  is non-leptophilic leading to sizable anti-proton excess in cosmic ray in contradiction with PAMELA data.

To explain the PAMELA data, one does not need to have a pure leptophilic model. A modified leptophilic model with sufficiently large lepton fraction with non-negligible hadron fraction in DM annihilation can be a viable model. Because the not completely negligible hadronic fraction, there may be some interesting testable consequences. The leptocentric  $U(1)_{B-3L_i}$  model [15] is an interesting example of this type.

The  $U(1)_{B-3L_i}$  model can be classified into three different models with  $L_i$  being: a)  $L_e$ , b)  $L_\mu$ , and c)  $L_\tau$ . Assuming the DM field  $\psi$  is a Dirac fermion which couples to  $Z'$  with a

charge  $a$ , the  $Z'$  coupling to SM fermions and DM are given by

$$L_{int} = Z'_\mu \left[ a g' \bar{\psi} \gamma^\mu \psi + \frac{1}{3} g' \sum_{j=u,d,c,s,t,b} \bar{q}_j \gamma^\mu q_j + 3 g' (\bar{l}_i \gamma^\mu l_i + \bar{\nu}_{L_i} \gamma^\mu \nu_{L_i} + \bar{\nu}_{R_i} \gamma^\mu \nu_{R_i}) \right], \quad (5)$$

where  $l_i$  and  $\nu_{L_i}$  are one of the lepton generations.  $\nu_{R_i}$  is the right handed neutrino which can be light (Dirac type of neutrino) or heavy (Majorana type of neutrino). To give a mass to  $Z'$ , the simplest way is to introduce a SM singlet Higgs boson  $S$  with non-trivial  $U(1)_{B-3L_i}$  charge  $b$ . After the singlet develops a non-zero vacuum expectation value  $\langle S \rangle = v_s/\sqrt{2}$ , the  $Z'$  mass  $m_{Z'}$  is given by  $m_{Z'}^2 = b^2 g'^2 v_s^2$ .

All of the three models a), b) and c) have suppressed hadronic DM annihilation fractions. This can be easily understood by noticing that the cross section of DM annihilate to quark final products  $\sigma$  is proportional to  $2 \times 3 \times 3 \times (g'/3)^2$  (the first factor 2 takes care of up and down sector, the first 3 is the number of quark generation, the second 3 is the number of color and last factor  $g'/3$  is the  $Z'$  coupling to quark), but to charged lepton is proportional to  $(3g')^2$ . Therefore the ratio of final products with quarks to final products with charged leptons is given by

$$R = \frac{\sigma(\sum_j q_j \bar{q}_j)}{\sigma(l_i \bar{l}_i)} = \frac{2}{9}. \quad (6)$$

Here we have assumed that the phase space with top quarks in the final states are approximately the same as other lighter quarks and leptons. This approximate is justified as the DM should have a mass of order TeV to cover the  $e^\pm$  excess energy range.

It is clear that this model has suppressed hadronic DM annihilation fraction, but non-zero at tree level. With the above suppressed hadronic fraction, all the above three models are allowed by the PAMELA data. But it is interesting to note, as will be shown later, that because the non-zero tree level cross section, just beyond the reach of the current PAMELA data these models predict noticeable anti-proton excesses. Therefore with higher experimental energy reach, these models will be tested. To further distinguish different models, one needs to consider more experimental constraints.

Without carrying out detailed numerical analysis one can make some judgments on favored models. Considerations from the  $e^\pm$  spectrum shape can help to select preferred models. To this end we note that model a) would predict a sharp falling in  $e^\pm$  energy around the DM mass because the DM annihilate directly into a pair of electron and positron through the  $Z'$  mediation. This model seems to be favored by the ATIC data, but

the more precise data from FERMI-LAT and HESS do not confirm the sharp falling feature and therefore disfavored this model. For models b) and c) the electron and positron are secondary final products from  $\mu^+\mu^-$  (model b)) and  $\tau^+\tau^-$  (model c)) after DM annihilation. The  $e^\pm$  spectrum is much more softer and are favored by FERMI-LAT and HESS data, but can not fit the ATIC data well.

Cosmic  $\gamma$  ray can further distinguish models a), b) and c). Model c having  $\tau^+\tau^-$  as the primary DM annihilation products has a large fraction in hadronic final state. There are a lot of  $\pi^0$  which can decay into  $\gamma$  pairs which leads to visible  $\gamma$  ray excesses at observable level. The present data from HESS disfavors this model. On the other hand, for models a) and b),  $\gamma$  ray dominantly comes from final state radiation. We will show that  $\gamma$  ray produced in this model is just below the current bound.

#### IV. THE $e^\pm$ COSMIC RAY

In the  $U(1)_{B-3L_i}$  model, the relic density of the dark matter is controlled by annihilation of  $\bar{\psi}\psi \rightarrow Z'^* \rightarrow \sum_j q_j \bar{q}_j + l_i \bar{l}_i + \nu_i \bar{\nu}_i$ , while the  $e^\pm$  excess is mainly determined by  $\bar{\psi}\psi \rightarrow Z'^* \rightarrow l_i \bar{l}_i$ . The interaction rate  $(\sigma v)_{l_i \bar{l}_i}$ , with the  $l_i$  mass neglected is given by

$$(\sigma v)_{l_i \bar{l}_i} = \frac{9}{\pi} \frac{a^2 g'^4 m_\psi^2}{(s - m_{Z'}^2)^2 + \Gamma_{Z'}^2 m_{Z'}^2}, \quad (7)$$

where  $v$  is the relative velocity of the two annihilating dark matter and  $s$  is the total DM pair energy squared in the center of mass frame.  $\Gamma_{Z'}$  is the decay width of the  $Z'$  boson. If the  $Z'$  mass is below the  $\bar{\psi}\psi$  threshold which we will assume, the dominant decay modes of  $Z'$  are  $Z' \rightarrow \sum_j q_j \bar{q}_j + l_i \bar{l}_i + \bar{\nu}_i \nu_i$ , and  $\Gamma_{Z'}$  is given by, neglecting final particle masses

$$\Gamma_{Z'} = \frac{31 g'^2}{24\pi} m_{Z'}. \quad (8)$$

The annihilation rate  $(\sigma v)_{relic}$  controlling the relic density is given by  $31(\sigma v)_{l_i \bar{l}_i}/18$ .

In the above, we have assumed that there are only left-handed light neutrinos. If there are light right-handed neutrinos to pair up with left-handed neutrinos to form Dirac neutrinos, the factor 31 in these equations should be changed to 40.

Since the relic density of DM is determined by the annihilation rate  $(\sigma v)_{relic}$ , the model parameters are thus constrained. The same parameters will also determine the annihilation rate producing the  $e^\pm$  excesses observed today, which requires a much larger annihilation

rate. A boost factor in the range 100 to 1000 is necessary. We find that Breit-Wigner resonance enhancement mechanism works very well in our models if the  $Z'$  boson mass is about two times of the dark matter mass [11, 13, 16].

The boost factor in this case comes from the fact that since the  $Z'$  mass  $m_{Z'}$  is close to two times of the dark matter mass  $m_\psi$ , the annihilation rate is close to the resonant point and is very sensitive to the thermal kinetic energy of dark matter. To see this let us rewrite the annihilation rate into a pair of charged leptons as

$$(\sigma v)_{l_i \bar{l}_i} = \frac{9a^2 g'^4}{16\pi m_\psi^2} \frac{1}{(\delta + v^2/4)^2 + \gamma^2}, \quad (9)$$

where we have used the non-relativistic limit of  $s = 4m_\psi^2 + m_\psi^2 v^2$ , with  $\delta$  and  $\gamma$  defined as  $m_{Z'}^2 = 4m_\psi^2(1 - \delta)$ , and  $\gamma^2 = \Gamma_{Z'}^2(1 - \delta)/4m_\psi^2$ .

For thermal dark matter, the velocity  $v^2$  is proportional to the thermal energy of dark matter. It is clear that for small enough  $\delta$  and  $\gamma$ , the annihilation rate is very sensitive to the thermal energy and therefore the thermal temperature  $T$ . At lower dark matter thermal energies, the annihilation rate is enhanced compared with that at higher temperature. This results in a very different picture of dark matter annihilation than the case for the usual non-resonant annihilation where the annihilation rate is not sensitive to dark matter thermal energies. The annihilation process does not freeze out even after the usual “freeze out” time in the non-resonant annihilation case due to the enhanced annihilation rate at lower energies. To produce the observed dark matter relic density, the annihilation rate at zero temperature is required to be larger than the usual one, and therefore a boost factor. With appropriate  $\delta$  and  $\gamma$ , a large enough boost factor can be produced. For our numerical analysis we follow the procedures in Ref.[13].

As already mentioned in the previous section that if  $l_i = e$ , the  $e^\pm$  is hard, but for  $l_i = \mu$  or  $\tau$ , the  $e^\pm$  have to come from  $\mu$  and  $\tau$  decays leading to softer  $e^\pm$  spectra.

In the Figs. 1 and 2 we show our results from fitting the PAMELA positron ratio and the ATIC or FERMI-LAT electron spectrum for the  $U(1)_{B-3L_e}$ ,  $U(1)_{B-3L_e}$  and  $U(1)_{B-3L_\tau}$  models taking the diffusion height  $Z_h$  4kpc and 2 kpc respectively.

There are several DM model parameters in the fitting, the DM mass  $m_D$ , the gauge coupling constant  $ag'^2$ . Since the Breit-Wigner enhancement for the boost factor forces the  $Z'$  mass  $m_{Z'}$  to be  $2m_D$ , it is not an independent parameter in the models we are considering. We find that the DM mass for  $L_i = e$ ,  $L_i = \mu$  and  $L_i = \tau$  are fixed to be in the ranges of

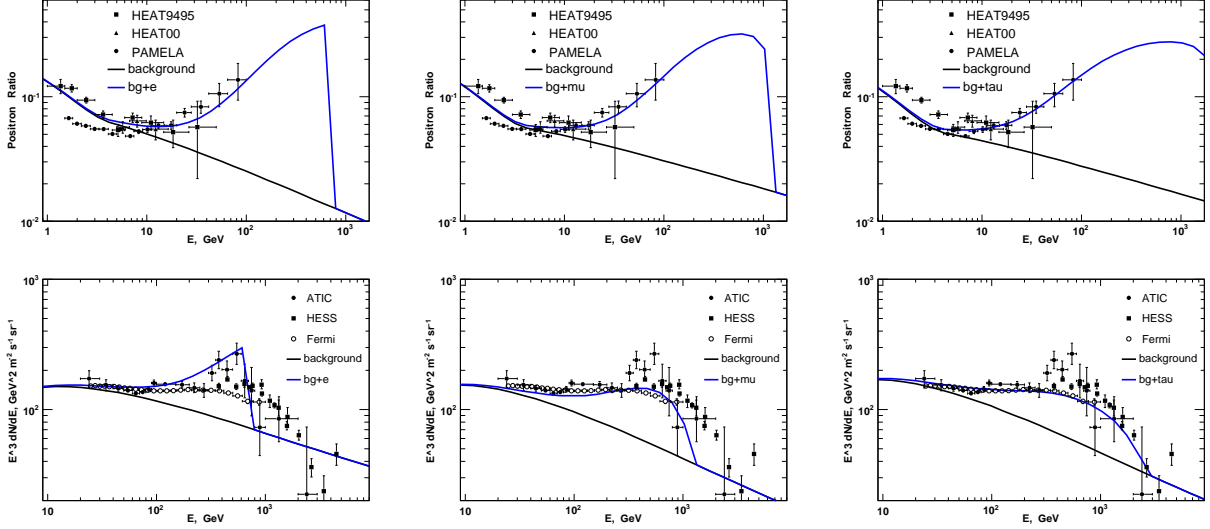


FIG. 1: The model prediction for  $e^\pm$  cosmic ray energy spectrum. The upper panels show the positron ratio to fit the PAMELA data with  $U(1)_{B-3L_i}$  models. The lower panels show the electron spectrum to fit the ATIC or Fermi data. The height of the Galactic diffusion region is taken as 4kpc.

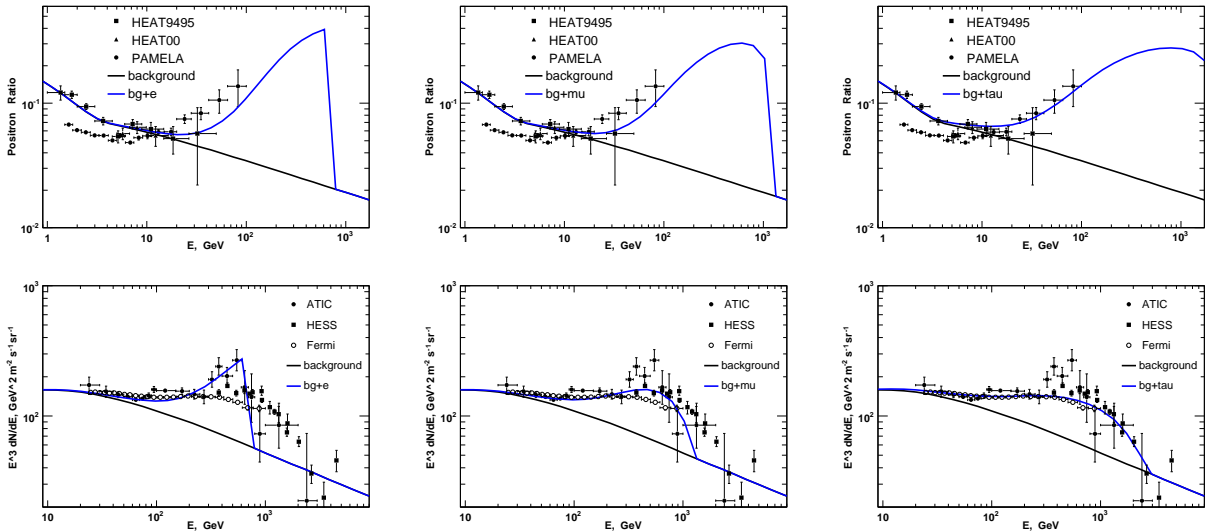


FIG. 2: The same as Fig. 1 except the height of the Galactic diffusion region taken as 2kpc.

several hundred GeV to several TeV in order to cover the observed ranges of  $e^\pm$  excesses. The corresponding values for  $ag'^2$  are limited to be of order  $10^{-5}$ . The masses and the coupling  $ag'^2$  used in the figures for three different models are 1 TeV, 1.5 TeV, 3 TeV, and  $1.7 \times 10^{-5}$ ,  $2.5 \times 10^{-5}$  and  $5.3 \times 10^{-5}$ , respectively.

To see how the astrophysics parameters affect the results, we show results for two different values for the height of the diffusion region. In Fig. 1 we have taken the height of the Galactic diffusion region as 4 kpc, while at Fig. 2 we take the height 2 kpc. We have adjusted the DM mass, the annihilation cross section to fit the data, and also the propagation parameters to account for all the cosmic ray data. For  $l_i = e$ , that is for the  $U(1)_{B-3L_e}$  model, the  $e^\pm$  spectra from DM annihilation are hard. With appropriate DM mass, from the figures we can see that this model can fit the PAMELA and ATIC data very well. For the other two models  $l_i = \mu$  (the  $U(1)_{B-3L_\mu}$  model) or  $l_i = \tau$  (the  $U(1)_{B-3L_\tau}$  model), the  $e^\pm$  spectra are from secondary decays of  $\mu$  or  $\tau$  and therefore are softer. It can be seen from the figures that these two models can fit the PAMELA and Fermi data. The  $U(1)_{B-3L_\tau}$  model has an even softer  $e^\pm$  spectra than those of the  $U(1)_{B-3L_\mu}$  model because  $\tau$  has large branching ratios into final states with no  $e$  in the final state.

## V. THE ANTI-PROTON COSMIC RAY

The anti-proton from DM annihilation in the  $U(1)_{B-3L_i}$  comes from DM annihilation into quark pairs whose annihilation rate is given by

$$(\sigma v)_{q\bar{q}} = \frac{1}{3\pi} \frac{a^2 g'^4 m_\psi^2}{(s - m_{Z'}^2)^2 + \Gamma_{Z'}^2 m_{Z'}^2}. \quad (10)$$

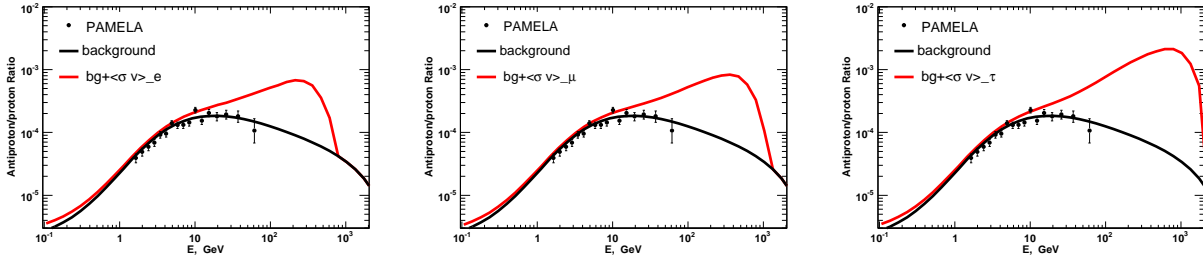


FIG. 3: The ratio of anti-proton to proton as function of energy predicted in the B-3e, B-3 $\mu$  and B-3 $\tau$  models respectively from the left to the right panels with  $Z_h = 4\text{kpc}$ . The cross section of DM annihilation is normalized to fit the ATIC or Fermi electron spectrum.

The quark and anti-quark produced from DM annihilation are subsequently fragmentate into hadrons and may cause excesses in cosmic proton and anti-proton spectra. In our analysis the anti-proton spectrum from quark pair hadronization is treated with the PYTHIA

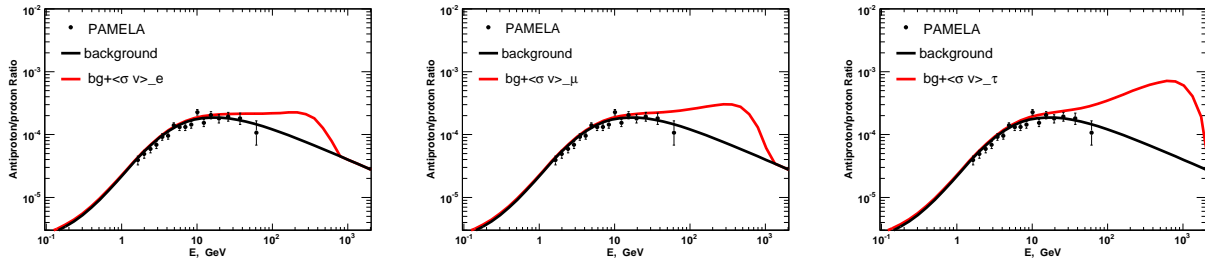


FIG. 4: The same as Fig. 3 but for  $Z_h = 2\text{kpc}$ .

package[26]. We find that different quark flavors have approximately the same proton and anti-proton spectra in the final products. Our results are shown in Fig. 3 and Fig. 4 with the diffuse height  $Z_h = 4\text{kpc}$  and  $2\text{kpc}$  respectively.

From the figures we see that at the high energy end of the anti-proton spectrum, there is already tension between the theoretical prediction and the current PAMELA data. For the diffusion height  $Z_h = 4\text{kpc}$  in Fig. 3 we notice that the antiproton fraction is obviously too much. However, due to large uncertainties in the propagation models, there are rooms to adjust parameters to fit the data. When we adopt the diffusion height  $Z_h = 2\text{kpc}$ , as shown in Fig. 4, the anti-proton flux is suppressed and the ratio is consistent with the PAMELA data at about  $2\sigma$  level. It should be noted that for both  $Z_h = 4\text{kpc}$  and  $Z_h = 2\text{kpc}$  we have adjusted the other propagation parameters, such as the diffusion coefficient  $D(E)$ , so that all the cosmic ray data are well reproduced in both models. The DM annihilation cross section are normalized so that the ATIC or Fermi electron spectrum is well fitted, as shown in Figs. 1 and 2.

We also notice from Figs. 3 and 4 that the contribution of anti-protons from DM annihilation is most important at several hundred GeV. Therefore future data at higher energies will give much more stringent constraints on the DM contribution to anti-protons. We expect that the near future PAMELA and AMS02 data will play a crucial role in testing different DM annihilation models.

## VI. THE $\gamma$ -RAY RADIATION FROM THE GALACTIC CENTER

Since we require a very large DM annihilation cross section to account for the observational  $e^\pm$  CR excesses, this will lead to a strong  $\gamma$ -ray radiation from the final lepton states,

i.e. via  $\psi\bar{\psi} \rightarrow Z' \rightarrow l_i\bar{l}_i\gamma$ . The cross section for high energy  $\gamma$  of energy  $E_\gamma$ , with  $m_\psi \gg m_{l_i}$ , is given by [27]

$$\frac{d\sigma_{l_i\bar{l}_i\gamma}}{dE_\gamma} = \sigma_{l_i\bar{l}_i} \frac{\alpha}{\pi} \frac{1}{E_\gamma} \left[ \ln \frac{s'}{m_\mu^2} - 1 \right] \left[ 1 + \frac{s'^2}{s^2} \right], \quad (11)$$

where  $s = 4m_\psi^2$  and  $s' = 4m_\psi(m_\psi - E_\gamma)$ . For the  $\tau$  final states more  $\gamma$ -rays will be produced from the  $\tau$  hadronic decays, which will be calculated using PYTHIA package[27]. We will calculate the  $\gamma$ -ray emission from the Galactic Center (GC) in the models under consideration and check if they are consistent with the HESS observation at the GC [28].

As can be seen from Eq. (3) that the  $\gamma$ -ray produced by DM annihilation depends on the square of the DM profile  $\rho$  and therefore the result will be sensitive to the form of  $\rho$ . In the following calculation we will take two popular dark matter density profiles, the NFW profile [29] and the Einasto profile [30], to predict the  $\gamma$ -ray flux for comparisons. The two density profiles take the forms as

$$\begin{aligned} \rho_{NFW}(r) &= \frac{\rho_s}{(r/r_s)(1+r/r_s)^2}, \\ \rho_{Eina}(r) &= \rho_0 \exp \left[ -\frac{2}{\alpha} \left( \frac{r^\alpha - R_\odot^\alpha}{r_s^\alpha} \right) \right], \end{aligned} \quad (12)$$

where we take the scale radius  $r_s = 25\text{kpc}$ ,  $\alpha = 0.23$  for the Einasto profile and normalize the local density as  $\rho_\odot = 0.3\text{GeV}/\text{cm}^3$ . Given the density profile, the  $\gamma$ -ray flux along a specific direction can be calculated as given in Eqs. (3) and (4).

We calculate the diffuse emission at the GC with the galactic latitude  $b$  and longitude  $l$  in the region  $|b| < 0.3^\circ$ ,  $|l| < 0.8^\circ$  and compare the result with the HESS observation [28]. To compare with spectra reported by HESS we have followed the HESS collaboration to subtract the background from  $0.8^\circ < |b| < 1.5^\circ$  [28].

In Fig. 5 we show the results together with the data taken from the HESS observation on the same region [28]. For the  $\tau$  final states we notice the  $\gamma$ -ray flux from GC is greatly higher than the observed one. Therefore the  $B-3\tau$  model is disfavored considering its  $\gamma$ -ray emission at the GC. Further,  $\gamma$ -rays also exceed the HESS result if taking the NFW profile no matter what the final states are taken. However, the recent high precision simulation show that the density profile at the halo center does not tend to any simple form of power law [31]. Instead the Einasto profile gives best fit to the most recent simulations [31, 32]. We also notice that if DM annihilates into electrons or muons the  $\gamma$ -ray flux is consistent with HESS when taking the Einasto profile.

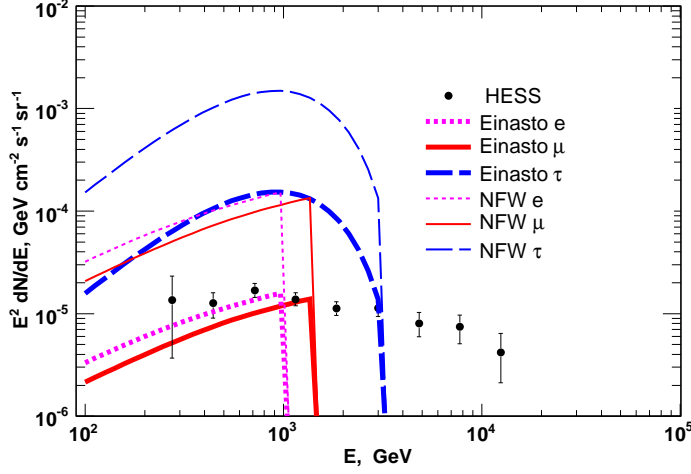


FIG. 5: The  $\gamma$ -ray emission from the GC region in the  $B - 3L_i$  models. The data are taken from the HESS observation at the same region [28]. We have taken NFW and Einasto profiles to predict the  $\gamma$ -ray fluxes.

It should be noted that for the two propagation models with  $Z_h = 4\text{kpc}$  and  $2\text{kpc}$  the  $\gamma$ -ray flux from the GC is almost the same, since the HESS observation focus on a very small region around the GC.

## VII. THE NEUTRINO COSMIC RAYS

In the  $U(1)_{B-3L_i}$  models, there are large fractions that DM annihilate into neutrino and anti-neutrino  $\nu_i \bar{\nu}_i$  pairs directly. The annihilation rate is given by

$$(\sigma v)_{\nu_i \bar{\nu}_i} = A \frac{9}{\pi} \frac{a^2 g'^4 m_\psi^2}{(s - m_{Z'}^2)^2 + \Gamma_{Z'}^2 m_{Z'}^2}, \quad (13)$$

where  $A = 1$  if the right- and left-handed neutrinos pair up to have Dirac mass, and  $A = 1/2$  if the right-handed neutrinos are heavy. This is a two body annihilation process and the neutrino energy spectrum produced will be line spectrum type. Therefore the line spectrum neutrinos, if detected, are distinctive signals of DM annihilation, since no astrophysical processes can produce such line spectrum.

There are also neutrinos from secondary decays of  $\mu \rightarrow \nu_\mu e \bar{\nu}_e$  for the  $U(1)_{B-3L_\mu}$  and  $\tau \rightarrow \nu_\tau \mu \bar{\nu}_\mu + \nu_\tau e \bar{\nu}_e$  for the  $U(1)_{B-3L_\tau}$  model.  $\tau$  can also produce softer neutrinos by hadronic decays. However, these continuous spectrum neutrinos are hard to be discriminated from

the atmospheric neutrino background. Further, taking these soft neutrinos into account we have to lower the threshold of the neutrino detector. The amount of atmospheric neutrinos increase rapidly by lowering energy since they have a very soft spectrum [33].

There have been some studies of detectability of neutrinos from the GC by DM annihilation [34]. As shown in the last section the  $B - 3\tau$  model has been excluded by the  $\gamma$ -ray emission. Therefore we calculate the neutrino fluxes in the cases of  $B - 3e$  and  $B - 3\mu$  with the Einasto profile which are consistent with the HESS  $\gamma$ -ray observation. We would like to check if the future IceCube observation can detect the neutrinos predicted by our models at the GC.

We will consider the muon neutrino detection rate at IceCube. The flavor eigenstates produced at the source will be modified at the detection point due to neutrino oscillations. The relation between different flavors from the GC to the Earth is given by [35]

$$(\phi_i)_{Earth} = P_{ij}(\phi_j)_{GC} , \quad (14)$$

where  $P_{ij}$  is the probability of converting the  $j$ -th flavor type of neutrino at the source to the  $i$ -th flavor neutrino at the detection point.

Assuming tri-bimaximal neutrino mixing pattern, the  $P_{ij}$  matrix after neutrinos traveling a galactic distance is given by

$$(P_{ij}) = \frac{1}{8} \begin{pmatrix} 8 - 4\omega & 2\omega & 2\omega \\ 2\omega & 4 - \omega & 4 - \omega \\ 2\omega & 4 - \omega & 4 - \omega \end{pmatrix} , \quad (15)$$

where  $\omega = \sin^2(2\theta_{12}) \approx 0.87$ . Since the tri-bimaximal mixing is a good approximation to present data, we will use the above formula for numerical estimate. We find that the muon neutrino fluxes arriving at the Earth are 0.22 and 0.4 times of the initial  $\nu_e$  and  $\nu_\mu$  fluxes at the sources, respectively.

We consider the detectability of the line neutrino spectrum of our models by the planned additional DeepCore within the IceCube detector. We take a conservative angular resolution as large as  $\pi$  Sr. Considering the contained events within the DeepCore it is not difficult to calculate the  $\nu_\mu$  events for 4 years observation with the DeepCore volume  $0.04\text{km}^3$ . The total contained muon events are about 606 for  $\nu_\mu$  initial flavor coming from the  $\pi$  solid angle centered at the GC when assuming the DM annihilation cross section is large enough to account

for the cosmic  $e^\pm$  anomalies and the Einasto density profile. Taking the energy resolution of the detector  $\sigma(\log_{10}(E)) \sim 0.4$  [36] (corresponding to the energy bin  $600\text{GeV} \sim 3.77\text{TeV}$ ) and taking the atmospheric neutrino background of [33] we get about 2350 contained background events at DeepCore/IceCube for 4 years observation from the GC direction for  $\pi$  Sr solid angle. About 68% signal events will fall within the  $1\sigma$  energy range. Then we find that the DeepCore/IceCube will be able to detect the line spectrum neutrinos at the confidence level  $8.5\sigma$  signal for 4 years observation with the  $B - 3\mu$  model, if the DM annihilation rate is fixed by the  $e^\pm$  excess data. For the  $B - 3e$  model (with the  $\nu_e$  initial flavor) the DM mass is 1TeV. Therefore the energy bin is from  $400\text{GeV}$  to  $2.5\text{TeV}$ . We then get the moun contained events for 4 years observation are about 243. The background events are much larger with about 4000 events since the energy bin is lower now. In this case we can only have a  $2.6\sigma$  signal for the  $\nu_e$  initial state which will oscillate into  $\nu_\mu$ .

Here we have taken a conservative angular resolution. Considering that the DeepCore may have a better angular resolution we may get signals with much higher significance. Therefore the neutrino events are very promising signals to test the DM annihilation model which explain the cosmic  $e^\pm$  excesses. If the scenario is correct we expect to detect at DeepCore/IceCube of the line spectrum neutrinos predicted in the  $B - 3L_i$  models.

### VIII. CONCLUSIONS

In this work we studied cosmic  $e^\pm$ ,  $\bar{p}$ ,  $\gamma$  and neutrino rays in the leptocentric  $U(1)_{B-3L_i}$  dark matter models. In these models, DM annihilation into SM particles is mediated by the  $Z'$  gauge boson of  $U(1)_{B-3L_i}$ . The couplings of  $Z'$  to leptons are larger than those to quarks leading to larger annihilation of DM to leptons than hadrons. This naturally explains the  $e^\pm$  excesses from PAMELA, ATIC or FERMI observational data, and at the same time these models can suppress the anti-proton flux efficiently. We find that the  $U(1)_{B-3L_e}$  model can fit PAMELA and ATIC, while  $U(1)_{B-3\mu}$  and  $U(1)_{B-3\tau}$  can fit PAMELA and FERMI, respectively. Future data can be used to distinguish different models. We showed that by slightly adjusting the propagation parameters these models can predict anti-proton flux consistent with the PAMELA data. But these models are different than pure leptophilic models which predict negligible anti-proton cosmic ray in all energy ranges, the leptocentric  $U(1)_{B-3L_i}$  models predict anti-proton flux beyond the background at higher energies which

can be tested by the near future data from PAMELA or AMS02.

The  $U(1)_{B-3L_i}$  models have predictions for cosmic  $\gamma$ -rays from DM annihilation. We investigated the  $\gamma$ -ray emission from the GC in these models. We found that the  $U(1)_{B-3\tau}$  model is excluded by the HESS observation of the GC region since this model predicts too much  $\gamma$ -rays. Adopting the Einasto DM density profile the other two models predict  $\gamma$ -rays consistent with HESS data.

We also investigated the detectability of neutrinos from the GC by the  $U(1)_{B-3e}$  and  $U(1)_{B-3\mu}$  models at DeepCore/IceCube. In these models the fraction of the DM annihilation into neutrinos are large and produce line spectrum neutrinos detectable by DeepCore/IceCube. We found that the DeepCore/IceCube can have a  $8.5(2.6)\sigma$  signal of the line neutrino spectrum for 4 years data taking. This will be a distinctive signal of DM annihilation in our leptocentric  $U(1)_{B-3e}$  and  $U(1)_{B-3\mu}$  models.

Finally we would like to have some comments on the detectability of leptocentric DM model at the LHC and direct DM detection experiments. Since the leptocentric DM models discussed here are very different than the pure leptophilic DM models, where the  $Z'$  only has interactions with leptons at the tree level, the  $Z'$  in our cases has interaction with quarks and may lead to detectable effects at the LHC and also direct DM search on the Earth. However because we rely on Breit-Wigner resonant enhancement effect to produce the large boost factor, the  $Z'$  mass is constrained to be 2 times of the DM mass and is constrained to be in the TeV range and the couplings  $ag'^2$  to be in the range of  $1 \times 10^{-5}$  to  $5 \times 10^{-5}$ , the cross section for producing  $Z'$  and virtual effects due to  $Z'$  for the LHC and also for direct detection are small, it is not possible to have observable effects at the LHC and near future direct DM detection experiments. To have a lower  $Z'$  mass and therefore to have observable effects at the LHC and direct DM detection experiments, a different mechanism for the boost factor has to be in effective to relax the relation that the  $Z'$  mass is about 2 times of the DM mass. To this end we note that if there is a long range interaction between DM by exchanging a light new particle, it is possible to have the Sommerfeld effect in operation, e.g. in Ref. [14, 37]. This offers another interesting possibility to explain the cosmic data. We will give details for this possibility elsewhere.

### Acknowledgments

We thank Yuan Qiang for helpful discussions in our calculations of  $\gamma$ -ray and neutrino emission. This work was supported in part by the NSF of China under grant No. 10773011, by the Chinese Academy of Sciences under the grant No. KJCX3-SYW-N2, by NSC and NCTS, and by the DOE under Grant No. DE-FG03-94ER40837..

- 
- [1] O. Adriani *et al.* [PAMELA Collaboration], *Nature* **458**, 607 (2009).
  - [2] O. Adriani *et al.*, *Phys. Rev. Lett.* **102**, 051101 (2009).
  - [3] S. W. Barwick *et al.* [HEAT Collaboration], *Astrophys. J.* **482**, L191 (1997).
  - [4] M. Aguilar *et al.* [AMS-01 Collaboration], *Phys. Lett. B* **646**, 145 (2007).
  - [5] J. Chang *et al.*, *Nature* **456**, 362 (2008).
  - [6] S. Torii *et al.*, arXiv:0809.0760 [astro-ph].
  - [7] A. A. Abdo *et al.* [The Fermi LAT Collaboration], *Phys. Rev. Lett.* **102**, 181101 (2009).
  - [8] F. Aharonian *et al.* [H.E.S.S. Collaboration], arXiv:0905.0105 [astro-ph.HE].
  - [9] F. Aharonian *et al.* [H.E.S.S. Collaboration], *Phys. Rev. Lett.* **101**, 261104 (2008).
  - [10] L. Bergstrom, T. Bringmann and J. Edsjo, *Phys. Rev. D* **78**, 103520 (2008) [arXiv:0808.3725 [astro-ph]]; V. Barger, W. Y. Keung, D. Marfatia and G. Shaughnessy, *Phys. Lett. B* **672**, 141 (2009) [arXiv:0809.0162 [hep-ph]]; C. R. Chen, F. Takahashi and T. T. Yanagida, *Phys. Lett. B* **671**, 71 (2009) [arXiv:0809.0792 [hep-ph]]; M. Cirelli, M. Kadastik, M. Raidal and A. Strumia, *Nucl. Phys. B* **813**, 1 (2009) [arXiv:0809.2409 [hep-ph]]. N. Arkani-Hamed, D. P. Finkbeiner, T. R. Slatyer and N. Weiner, *Phys. Rev. D* **79**, 015014 (2009) [arXiv:0810.0713 [hep-ph]]. Y. Bai and Z. Han, *Phys. Rev. D* **79**, 095023 (2009) [arXiv:0811.0387 [hep-ph]]; E. J. Chun and J. C. Park, *JCAP* **0902**, 026 (2009) [arXiv:0812.0308 [hep-ph]]; J. Zhang, X.-J. Bi, J. Liu, S.-M. Liu, P.-F. Yin, Q. Yuan, S.-H. Zhu, *Phys. Rev. D* **80**, 023007 (2009) [arXiv:0812.0522 [astro-ph]]; J. Liu, P. f. Yin and S. h. Zhu, arXiv:0812.0964 [astro-ph]; C. H. Chen, C. Q. Geng and D. V. Zhuridov, arXiv:0901.2681 [hep-ph]; X. J. Bi, P. H. Gu, T. Li and X. Zhang, *JHEP* **0904**, 103 (2009) [arXiv:0901.0176 [hep-ph]]; S. Khalil, H. S. Lee and E. Ma, *Phys. Rev. D* **79**, 041701R (2009) [arXiv:0901.0981 [hep-ph]]; Q. H. Cao, E. Ma and G. Shaughnessy, *Phys. Lett. B* **673**, 152 (2009) [arXiv:0901.1334 [hep-ph]]; K. Cheung, P. Y. Tseng and T. C. Yuan,

- Phys. Lett. B **678**, 293 (2009) [arXiv:0902.4035 [hep-ph]]; S. L. Chen, R. N. Mohapatra, S. Nussinov and Y. Zhang, Phys. Lett. B **677**, 311 (2009) [arXiv:0903.2562 [hep-ph]]; B. Dutta, L. Leblond and K. Sinha, arXiv:0904.3773 [hep-ph]; X. J. Bi, R. Brandenberger, P. Gondolo, T. j. Li, Q. Yuan and X. m. Zhang, arXiv:0905.1253 [hep-ph]; C. H. Chen, C. Q. Geng and D. V. Zhuridov, arXiv:0905.0652 [hep-ph]; Q. Yuan, X.-J. Bi, J. Liu, P.-F. Yin, J. Zhang, S.-H. Zhu, arXiv:0905.2736 [astro-ph.HE]; C. H. Chen, arXiv:0905.3425 [hep-ph]; J. Liu, Q. Yuan, X.-J. Bi, H. Li and X. Zhang, arXiv:0906.3858 [astro-ph.CO]. P. H. Gu, H. J. He, U. Sarkar and X. m. Zhang, arXiv:0906.0442 [hep-ph]. C. H. I. Chen, C. Q. I. Geng and D. V. Zhuridov, arXiv:0906.1646 [hep-ph]; J. Zhang, Q. Yuan, X.-J. Bi, arXiv:0908.1236 [astro-ph.HE].
- [11] D. Feldman, Z. Liu and P. Nath, Phys. Rev. D **79**, 063509 (2009) [arXiv:0810.5762 [hep-ph]].
- [12] P. J. Fox and E. Poppitz, Phys. Rev. D **79**, 083528 (2009) [arXiv:0811.0399 [hep-ph]]; S. Baek and P. Ko, arXiv:0811.1646 [hep-ph]; H. S. Goh, L. J. Hall and P. Kumar, JHEP **0905**, 097 (2009) [arXiv:0902.0814 [hep-ph]]; H. Davoudiasl, arXiv:0904.3103 [hep-ph];
- [13] X. J. Bi, X. G. He and Q. Yuan, Phys. Lett. **B678**, 168 (2009).
- [14] For a brief review of the dark matter annihilation for cosmic  $e^\pm$  excesses, see Xiao-Gang He, Mod. Phys. Lett. **A24**, 2139(2009)[arXiv:0908:2908[hep-ph]]
- [15] E. Ma, Phys. Lett. B **433**, 74 (1998); E. Ma and D. P. Roy, Phys. Rev. D **58**, 095005 (1998); E. Ma and U. Sarkar, Phys. Lett. B **439**, 95 (1998).
- [16] M. Ibe, H. Murayama and T. T. Yanagida, Phys. Rev. D **79**, 095009 (2009) [arXiv:0812.0072 [hep-ph]]. W. L. Guo and Y. L. Wu, Phys. Rev. D **79**, 055012 (2009) [arXiv:0901.1450 [hep-ph]].
- [17] T.K. Gaisser, *Cambridge, UK: Univ. Pr. (1990) 279 p*
- [18] A. W. Strong and I. V. Moskalenko, Astrophys. J. **509**, 212 (1998). [arXiv:astro-ph/9807150]. I. V. Moskalenko and A. W. Strong, Astrophys. J. **493**, 694 (1998). [arXiv:astro-ph/9710124].
- [19] P. F. Yin, Q. Yuan, J. Liu, J. Zhang, X. J. Bi, S. H. Zhu and X. M. Zhang, arXiv:0811.0176 [hep-ph].
- [20] E. S. Seo and V. S. Ptuskin, Astrophys. J. **431**, 705 (1994)
- [21] I. V. Moskalenko, A. W. Strong, J. F. Ormes and M. S. Potgieter, Astrophys. J. **565**, 280 (2002). [arXiv:astro-ph/0106567].
- [22] A. W. Strong, I. V. Moskalenko and O. Reimer, Astrophys. J. **537**, 763 (2000) [Erratum-ibid. **541**, 1109 (2000)]. [arXiv:astro-ph/9811296].

- [23] A. W. Strong, I. V. Moskalenko and O. Reimer, *Astrophys. J.* **613**, 962 (2004).  
[arXiv:astro-ph/0406254].
- [24] F. Donato, N. Fornengo, D. Maurin, P. Salati, *Phys. Rev. D* **69**, 063501 (2004).
- [25] T. Delahaye, F. Donato, N. Fornengo, J. Lavalle, R. Lineros, P. Salati, R. Taillet, *Astron. and Astrop.* **501**, 821 (2009).
- [26] T. Sjostrand, S. Mrenna and P. Skands, *JHEP* **0605**, 026 (2006) [arXiv:hep-ph/0603175].
- [27] L. Bergstrom, T. Bringmann, M. Eriksson and M. Gustafsson, *Phys. Rev. Lett.* **94**, 131301 (2005) [arXiv:astro-ph/0410359]; N. Fornengo, L. Pieri and S. Scopel, *Phys. Rev. D* **70**, 103529 (2004) [arXiv:hep-ph/0407342]; J. F. Beacom, N. F. Bell and G. Bertone, *Phys. Rev. Lett.* **94**, 171301 (2005) [arXiv:astro-ph/0409403].
- [28] F. Aharonian *et al.* [H.E.S.S. Collaboration], *Nature* **439**, 695 (2006) [arXiv:astro-ph/0603021].
- [29] J.F. Navarro, C.S. Frenk, S.D.M. White, *Astrophys. J.* **490**, 493 (1997).
- [30] J. Einasto, *Trudy Inst. Astrofiz. Alma-Ata* **51**, 87 (1965)
- [31] J. F. Navarro, A. Ludlow, V. Springel, J. Wang, M. Vogelsberger, S. D.M. White, A. Jenkins, C. S. Frenk, A. Helmi, arXiv:0810.1522v2 [astro-ph]; M. Boylan-Kolchin, V. Springel, S. D.M. White, A. Jenkins, G. Lemson, arXiv:0903.3041 [astro-ph.CO].
- [32] A. W. Graham, D. Merritt, B. Moore, J. Diemand, B. Terzic, *Astron. J.* **132**, 2701 (2006).
- [33] M. Honda, T. Kajita, K. Kasahara, S. Midorikawa and T. Sanuki, *Phys. Rev. D* **75**, 043006 (2007).
- [34] J. Liu, P.F. Yin, S.H. Zhu, *Phys. Rev. D* **79**, 063522 (2009); D. Spolyar, M. Buckley, K. Freese, D. Hooper, H. Murayama, arXiv:0905.4764v1 [astro-ph.CO].
- [35] S. Pakvasa, W. Rodejohann and T. J. Weiler, *JHEP* **0802**, 005 (2008) [arXiv:0711.4517 [hep-ph]]; K.-C. Lai, G.-L. Lin, T. C. Liu, arXiv:0905.4003.
- [36] E. Resconi and F.T.I. Collaboration, *Nucl. Instrum. Meth. A* **602**, 7 (2009) [arXiv: 0807.3891].
- [37] J. Hisano, S. Matsumoto and M. M. Nojiri, *Phys. Rev. Lett.* **92**, 031303 (2004) [arXiv:hep-ph/0307216].